REPORT NO.
UCB/SEMM-90/16

STRUCTURAL ENGINEERING
MECHANICS AND MATERIALS

A HYBRID QUADRILATERAL PLATE BENDING ELEMENT FOR THE INCLUSION OF WARPING BASED ON A THREE-DIMENSIONAL PLATE FORMULATION

BY

R. PILTNER

AUGUST 1990

DEPARTMENT OF CIVIL ENGINEERING
UNIVERSITY OF CALIFORNIA
BERKELEY, CALIFORNIA

A HYBRID QUADRILATERAL PLATE BENDING ELEMENT FOR THE INCLUSION OF WARPING BASED ON A THREE-DIMENSIONAL PLATE FORMULATION

R. PILTNER

Department of Civil Engineering, University of California at Berkeley,

Berkeley, CA 94720, U.S.A.

SUMMARY

A plate formulation for the inclusion of warping and transverse shear deformations is considered. From a complete thick and thin plate formulation, which was derived without ad hoc assumptions from the three-dimensional equations of elasticity for isotropic materials, the bending solution, involving powers of the thickness coordinate z, is used for constructing a quadrilateral finite plate bending element. The constructed element trial functions, for the displacements and stresses, satisfy a priori the 3-dimensional Navier-equations and equilibrium equations, respectively. For the coupling of the elements, independently assumed functions on the boundary are used. High accuracy for both displacements and stresses (including transverse shear stresses) can be achieved with rather coarse meshes for thick and thin plates.

1. INTRODUCTION

Although the research on plate formulations and solutions has existed for more than 140 years, a look at the recent literature shows that there are still possibilities for alternative formulations and improving techniques [1-37]. The purpose of this paper is to give an additional point of view on the solution of plate bending problems.

Plate theories are usually based on assumptions on stress, strain or displacement distributions over the thickness of the plate [38-42]. However, these assumptions unfortunately lead to inconsistencies in the plate theories. Assuming the displacement components u and v vary linearly and the transverse displacement w is constant over the thickness of the plate, we can not get a parabolic form for the shear stresses τ_{xz}, τ_{yz} in the thickness direction. Therefore,

from the constitutive equations, we do not get transverse shear distributions which satisfy the stress boundary conditions on the upper and lower plate faces.

The assumptions in the mentioned plate theories basically exclude the possibility of warping and thickness changes. However, the transverse shear stresses come from the warping and change of thickness terms, as it can be seen from the representations given in references [43,44] or from the summary of the main results given below. So when we are looking for plate solutions, which very accurately include transverse shear deformations and on the contrary neglect the warping and change of thickness terms, which cause the transverse shears, we are left with a basic contradiction.

Dealing with numerical approximations, one can ask whether it is possible to include the effects of warping and thickness changes in plate formulations in a simple way. In reference [43], a derivation of a thick and thin plate formulation without ad hoc assumptions was considered. Membrane and bending solution parts for plates were analyzed separately.

For the analysis in this paper we want to consider only bending solution contributions. This implies the assumption that the transverse loaded plate under consideration involves only minor membrane solution terms. After a summary of different types of bending solutions, taken from reference [43], a simplified plate theory for the inclusion of warping and transverse shear deformations is given. Then the variational formulation and the discretization for a hybrid finite element is discussed. From the literature on hybrid finite elements (see e.g. [7,45-48]) especially the pioneering work of Pian [49-52] has to be emphasized. Since the trial functions for the considered hybrid plate element satisfy the governing differential equations, the concept used for the proposed plate bending element can also be seen as Trefftz-method [53-67]. (Taking this point of view one could classify for example the hybrid crack element of Tong/Pian/Lasry [68] as a hybrid Trefftz-element.)

The numerical examples include the analysis of a 3-dimensional plate model for which the exact solution is known. The exact 3-dimensional solution is used to study the accuracy of the numerical results obtained with the proposed plate element.

2. THREE-DIMENSIONAL PLATE BENDING SOLUTION REPRESENTATIONS

The solution of the Navier-equations can be decomposed into a homogeneous solution and a

nonhomogeneous solution, where the nonhomogeneous solution takes nonvanishing body forces into account. The homogeneous bending solution, with powers of the thickness coordinate z, can be written as [43]

$$
\begin{aligned}
2\mu u &= -z\,\frac{\partial}{\partial x}G - \frac{1}{4(1-\nu)}\left[\,h^2 z - 2(2-\nu)\frac{z^3}{3}\,\right]\frac{\partial}{\partial x}\Delta G,\\
2\mu v &= -z\,\frac{\partial}{\partial y}G - \frac{1}{4(1-\nu)}\left[\,h^2 z - 2(2-\nu)\frac{z^3}{3}\,\right]\frac{\partial}{\partial y}\Delta G,\\
2\mu w &= G + \frac{\nu}{2(1-\nu)}z^2\,\Delta G,
\end{aligned}
\tag{1}
$$

where $G(x,y)$ has to satisfy $\Delta\Delta G = 0$ and $2\mu = E/(1+\nu)$. The displacement field (1) satisfies both the three-dimensional homogeneous Navier-equations and the homogeneous stress boundary conditions on the upper and lower faces of the plate (i.e. on $z = \pm h/2$). The second homogeneous solution part can be written as [43]

$$
\begin{aligned}
2\mu u &= \frac{\partial g_n}{\partial y}\sin\omega_n z,\\
2\mu v &= -\frac{\partial g_n}{\partial x}\sin\omega_n z,\\
2\mu w &= 0,
\end{aligned}
\tag{2}
$$

where $g_n(x,y)$ has to satisfy $\Delta g_n - \omega_n^2 g_n = 0$ and $\omega_n = n\pi/h \quad (n=1,3,5,\ldots.)$.

The third homogeneous solution part is [43]

$$
\begin{aligned}
2\mu u &= -\hat{G}_x\,[\,a\,\hat{z}\cosh q\hat{z} + b\,\hat{z}\sinh q\hat{z} + c\cosh q\hat{z} + d\sinh q\hat{z}\,],\\
2\mu v &= -\hat{G}_y\,[\,a\,\hat{z}\cosh q\hat{z} + b\,\hat{z}\sinh q\hat{z} + c\cosh q\hat{z} + d\sinh q\hat{z}\,],\\
2\mu w &= \hat{G}\,[\,a\left\{(3-4\nu)\cosh q\hat{z} - q\hat{z}\sinh q\hat{z}\right\} + b\left\{(3-4\nu)\sinh q\hat{z} - q\hat{z}\cosh q\hat{z}\right\}\\
&\qquad - c\,q\sinh q\hat{z} - d\,q\cosh q\hat{z}\,],
\end{aligned}
\tag{3}
$$

where $\hat{G}(x,y)$ has to satisfy $\Delta\hat{G} + q^2\hat{G} = 0$ and $\hat{z}=z+h/2$. From the stress free boundary conditions on the upper and lower plate faces, the characteristic equation $qh - \sinh qh = 0$ is derived and used to obtain an infinite series of complex eigenvalues. For every eigenvalue q, one can compute the according eigenvector $[a, b, c, d]^T$.

In addition to the solution parts satisfying homogeneous stress boundary conditions on the upper and lower plate faces, we need a solution part for the nonhomogeneous stress boundary conditions. These particular solutions for chosen load distributions can be constructed with the

aid of a function g(x,y), which satisfies the higher order differential equation $\Delta^n g = 0$. The value of n depends on the order of the load function. For the example of a constant normal load on the upper face of the plate, the solution is obtained from a function g(x,y), which satisfies $\Delta\Delta\Delta g = 0$, and is given in the next paragraph.

More details as well as the derivation of a nonhomogeneous solution of the Navier-equations for plate bending (in the case of a constant body force acting in the thickness direction) are given in reference [43].

The three-dimensional solution representations, briefly described above, can be used for numerical approximations. In order to get a finite element algorithm for plate bending with warping, the three-dimensional solution representations are reduced to a simplified plate theory, which is discussed in the following paragraph.

3. A SIMPLIFIED PLATE THEORY FOR THE INCLUSION OF WARPING

The only assumption for this theory is that for a plate bending problem the major solution contributions can be sufficiently approximated by the solution terms involving powers of the thickness coordinate z. The homogeneous solution part of this type can be written as [43]

$$
\begin{aligned}
2\mu u &= -z\frac{\partial}{\partial x}G - \frac{1}{4(1-\nu)}\left[\, h^2 z - 2(2-\nu)\frac{z^3}{3}\,\right]\frac{\partial}{\partial x}\Delta G,\\
2\mu v &= -z\frac{\partial}{\partial y}G - \frac{1}{4(1-\nu)}\left[\, h^2 z - 2(2-\nu)\frac{z^3}{3}\,\right]\frac{\partial}{\partial y}\Delta G,\\
2\mu w &= G + \frac{\nu}{2(1-\nu)}z^2\,\Delta G,\\
\sigma_{xx} &= -\frac{1}{1-\nu}z\left[\, G_{xx} + \nu G_{yy}\,\right] - \frac{1}{4(1-\nu)}\left[\, h^2 z - 2(2-\nu)\frac{z^3}{3}\,\right]\frac{\partial^2}{\partial x^2}\Delta G,\\
\sigma_{yy} &= -\frac{1}{1-\nu}z\left[\, G_{yy} + \nu G_{xx}\,\right] - \frac{1}{4(1-\nu)}\left[\, h^2 z - 2(2-\nu)\frac{z^3}{3}\,\right]\frac{\partial^2}{\partial y^2}\Delta G,\\
\sigma_{zz} &= 0,\\
\tau_{xy} &= -zG_{xy} - \frac{1}{4(1-\nu)}\left[\, h^2 z - 2(2-\nu)\frac{z^3}{3}\,\right]\frac{\partial^2}{\partial x\partial y}\Delta G,\\
\tau_{xz} &= \frac{1}{2(1-\nu)}\left[\, z^2 - \frac{h^2}{4}\,\right]\frac{\partial}{\partial x}\Delta G,\\
\tau_{yz} &= \frac{1}{2(1-\nu)}\left[\, z^2 - \frac{h^2}{4}\,\right]\frac{\partial}{\partial y}\Delta G,
\end{aligned}
\qquad (4)
$$

where G(x,y) has to satisfy

$$\Delta\Delta G = 0. \tag{5}$$

If we neglect in the representation (4) all terms which involve h^2, z^2, z^3, we get with $G(x,y)/(2\mu) = w(x,y)$ the relations for the Kirchhoff-plate theory.

In order to make a comparison with the Reissner-Mindlin-type of displacement fields used for finite elements, we write the displacement field of relationships (4) in the form

$$\begin{aligned} u &= -z\,\Theta_x + z^3 \frac{2-\nu}{2(1-\nu)} \frac{\partial}{\partial x}\Delta W(x,y), \\ v &= -z\,\Theta_y + z^3 \frac{2-\nu}{2(1-\nu)} \frac{\partial}{\partial y}\Delta W(x,y), \\ w &= W(x,y) + \frac{\nu}{2(1-\nu)} z^2\,\Delta W(x,y), \end{aligned} \tag{6}$$

where the substitutions

$$\Theta(x,y) = \frac{1}{2\mu}\left[\, G(x,y) + \frac{h^2}{4(1-\nu)}\,\Delta G(x,y)\,\right] \tag{7}$$

and

$$W(x,y) = \frac{G(x,y)}{2\mu} \tag{8}$$

have been used. Using Reissner-Mindlin displacement fields of the form $u = -z\,\Theta_x(x,y)$, $v = -z\,\Theta_y(x,y)$ and $w = W(x,y)$, we cannot obtain parabolic transverse shear distributions in the thickness direction from the constitutive equations $\sigma = E\,\epsilon = E\,D\,u$ since u and v are only linear in z. The formulation used in this paper includes higher order terms in z and provides, through the constitutive equations, parabolic transverse shear distributions over the thickness.

Using the displacement representation of relationships (4), we include the effects of warping and thickness changes. The evaluation of the transverse shear stresses from

$$\begin{aligned} \tau_{xz} &= 2\mu(u_z + w_x) \\ \tau_{yz} &= 2\mu(v_z + w_y) \end{aligned} \tag{9}$$

shows that the parabolic transverse shear distributions get their contributions from the warping and change of thickness functions, whereas the Kirchhoff-type of displacement field $2\mu u = -zG_x$, $2\mu v = -zG_y$, $2\mu w = G$ gives zero stresses τ_{xz} and τ_{yz}, if computed from the constitutive relationships (9).

For the function G(x,y) in the solution representation (4), a set of linearly independent approximation functions can be constructed and used for numerical computations. For a finite element, the use of trial functions for G(x,y) will result in an element stiffness matrix.

In addition to the solution part (4) we need a particular homogeneous solution part for nonhomogeneous boundary conditions on the upper or lower plate face and/or a particular solution for the inclusion of a body force. A particular homogeneous solution for a constant normal load p on the upper plate face can be given as [43]:

$$2\mu u = \frac{p\,x}{4h^3}\left[\,(2-\nu)(4z^3 - 3h^2 z) - 3(1-\nu)(x^2 + y^2)z + \frac{2\nu h^3}{1+\nu}\,\right],$$

$$2\mu v = \frac{p\,y}{4h^3}\left[\,(2-\nu)(4z^3 - 3h^2 z) - 3(1-\nu)(x^2 + y^2)z + \frac{2\nu h^3}{1+\nu}\,\right],$$

$$2\mu w = \frac{p}{16h^3}\left[\,-8(1+\nu)z^4 + 24\nu(x^2 + y^2)z^2 + 12h^2\,(1+\nu)z^2 + 3(1-\nu)(x^2 + y^2)^2 - 6h^2\,\nu(x^2 + y^2) - \frac{8h^3}{1+\nu}z\,\right],$$

$$\sigma_{xx} = \frac{p}{4h^3}\left[\,4(2+\nu)z^3 - (9+3\nu)x^2 z - (3+9\nu)y^2 z - 3h^2(2+\nu)z\,\right], \qquad (10)$$

$$\sigma_{yy} = \frac{p}{4h^3}\left[\,4(2+\nu)z^3 - (3+9\nu)x^2 z - (9+3\nu)y^2 z - 3h^2(2+\nu)z\,\right],$$

$$\sigma_{zz} = -\frac{p}{2h^3}(z + h)(2z - h)^2,$$

$$\tau_{xy} = -\frac{3p}{2h^3}(1-\nu)xyz,$$

$$\tau_{xz} = \frac{3p}{4h^3}x(2z - h)(2z + h),$$

$$\tau_{yz} = \frac{3p}{4h^3}y(2z - h)(2z + h).$$

For a constant body force $\bar{f}_z$ acting in the thickness direction, the following displacement field has been derived [43]:

$$2\mu u = \frac{\bar{f}_z}{4h^2}\left[\,4(2-\nu)z^3 - 3(1-\nu)(x^2 + y^2)z - 2h^2(1-\nu)z\,\right]x,$$

$$2\mu v = \frac{\bar{f}_z}{4h^2}\left[\,4(2-\nu)z^3 - 3(1-\nu)(x^2 + y^2)z - 2h^2(1-\nu)z\,\right]y, \qquad (11)$$

$$2\mu w = \frac{\bar{f}_z}{16h^2}\left[\,-8(1+\nu)z^4 + 24\nu(x^2 + y^2)z^2 + 4h^2(1+\nu)z^2\right.$$

$$- 2h^2(1+\nu)(x^2 + y^2) + 3(1-\nu)(x^2 + y^2)^2],$$

The particular solutions contain no free parameters and lead to an element load vector in a finite element algorithm. Other particular solutions can be derived. The construction of particular solutions is discussed in detail in reference [43]. In this paper, the particular solution (10) is used for illustrating the calculation of the element load vector.

4. VARIATIONAL FORMULATION

For the hybrid plate element considered in this paper, the following extended three-dimensional displacement functional is used for an element i:

$$\Pi_H^i = \Pi^i + \int_{S_u^i} \mathbf{T}^T (\tilde{\mathbf{u}} - \mathbf{u})\, dS^i \tag{12}$$

where

$$\Pi^i = \int_{V^i} [\, \frac{1}{2}(\mathbf{u}^T \mathbf{D}^T)\, \mathbf{E}\, (\mathbf{D}\mathbf{u}) - \mathbf{u}^T \bar{\mathbf{F}}\,]\, dV^i - \int_{S_T^i} \mathbf{u}^T \bar{\mathbf{T}}\, dS^i \tag{13}$$

and

$$\begin{aligned} \mathbf{u}^T &= [\, u, v, w\,] \\ \tilde{\mathbf{u}}^T &= [\, \tilde{u}, \tilde{v}, \tilde{w}\,] \\ \mathbf{T}^T &= [\, T_x, T_y, T_z\,]. \end{aligned} \tag{14}$$

In this matrix notation, $\mathbf{u}$ is the displacement field for the volume V^i of element i; $\mathbf{D}$ is a differential operator matrix; $\mathbf{E}$ contains the elastic constants; $\bar{\mathbf{F}}$ is a vector of given body forces; $\bar{\mathbf{T}}$ is the vector of prescribed tractions on the surface boundary portion S_T^i; and $\tilde{\mathbf{u}}$ is a vector of independently assumed boundary displacements, which are used for the coupling of elements along the boundary portion S_u^i and which are the same for two adjacent elements over their common boundary.

In order to simplify the variational formulation, the displacement field $\mathbf{u}$ is decomposed into a homogeneous solution part $\mathbf{u_h}$ and a particular solution part $\mathbf{u_p}$ according to

$$\mathbf{u} = \mathbf{u_h} + \mathbf{u_p}. \tag{15}$$

For $\mathbf{u_h}$ we will use functions constructed from the representation (4), whereas for $\mathbf{u_p}$ (depending on the loading) we can choose, for example, the functions given with relationships (10) or (11).

The field $\mathbf{u_h}$ contains linear independent trial functions with free parameters, whereas there are no free parameters in $\mathbf{u_p}$.

The tractions $\mathbf{T}$ on the element boundary are related to the strains $\mathbf{Du}$ and the stresses σ, respectively, through the relationship

$$\mathbf{T} = \mathbf{nEDu} = \mathbf{n}\sigma, \tag{16}$$

where $\mathbf{n}$ is the matrix of unit normals on the boundary. From the decomposition of the displacement field (15) follows the decomposition of the tractions, which can be written as

$$\mathbf{T} = \mathbf{T_h} + \mathbf{T_p}, \tag{17}$$

where $\mathbf{T_h} = \mathbf{nEDu_h}$ and $\mathbf{T_p} = \mathbf{nEDu_p}$.

In order to get a simplified expression for the functional (12) we integrate Π_H^i by parts to obtain:

$$\begin{aligned}
\Pi_H^i = & -\int_{V^i} \frac{1}{2}\mathbf{u_h^T}\,[\mathbf{D^T E D u_h}]\,dV^i + \int_{S^i} \frac{1}{2}\mathbf{u_h^T}\,[\mathbf{nEDu_h}]\,dS^i \\
& -\int_{V^i} \frac{1}{2}\mathbf{u_h^T}\,[\mathbf{D^T E D u_p} + \bar{\mathbf{F}}]\,dV^i + \int_{S^i} \mathbf{u_h^T}\,[\mathbf{nEDu_p}]\,dS^i \\
& -\int_{V^i} \frac{1}{2}\mathbf{u_p^T}\,[\mathbf{D^T E D u_p}]\,dV^i + \int_{S^i} \frac{1}{2}\mathbf{u_p^T}\,[\mathbf{nEDu_p}]\,dS^i \\
& -\int_{V^i} \mathbf{u_p^T}\bar{\mathbf{F}}\,dV^i - \int_{S_T^i} \mathbf{u_h^T}\bar{\mathbf{T}}\,dS^i - \int_{S_T^i} \mathbf{u_p^T}\bar{\mathbf{T}}\,dS^i \\
& +\int_{S_u^i} \mathbf{T^T}\,(\tilde{\mathbf{u}} - \mathbf{u})\,dS^i.
\end{aligned} \tag{18}$$

The boundary of the three-dimensional plate element is the surface S^i. The surface S^i is decomposed into two portions according to

$$S^i = S_u^i + S_T^i, \tag{19}$$

where S_T^i consists of the upper and lower faces of the plate where tractions $\bar{\mathbf{T}}$ are prescribed, and S_u^i consists of the lateral faces of the plate. Note that $\tilde{\mathbf{u}}$ is assumed on S_u^i. On those portions of S_u^i, which lie on parts of the boundary of the discretized structure, where displacements $\bar{\mathbf{u}}$ are prescribed, we will set $\tilde{\mathbf{u}} = \bar{\mathbf{u}}$.

The constructed displacement field $\mathbf{u}$ satisfies the Navier-equations

$$\mathbf{D}^T\mathbf{E}\mathbf{D}\mathbf{u} = -\bar{\mathbf{F}}, \tag{20}$$

and due to the decomposition of the displacements $\mathbf{u}$ into $\mathbf{u}_h$ and $\mathbf{u}_p$ we have the properties

$$\mathbf{D}^T\mathbf{E}\mathbf{D}\mathbf{u}_h = -\mathbf{0}, \tag{21}$$

$$\mathbf{D}^T\mathbf{E}\mathbf{D}\mathbf{u}_p = -\bar{\mathbf{F}}. \tag{22}$$

The substitution of relationships (21) and (22) into (18) eliminates two volume integrals. Further simplifications for the functional Π_H^i are possible since the satisfaction of the boundary condition

$$\mathbf{T} = \bar{\mathbf{T}} \quad \text{on } S_T^i \ \text{(i.e. } z = \pm h/2) \tag{23}$$

is also a priori ensured. Using the decomposition (17), our functions have the properties

$$\mathbf{T}_h = \mathbf{0} \quad \text{on } S_T^i \tag{24}$$

$$\mathbf{T}_p = \bar{\mathbf{T}} \quad \text{on } S_T^i. \tag{25}$$

Using the properties (21), (22), (24) and (25) the functional Π_H^i of relationship (18) can be written as

$$\Pi_H^i = -\int_{S_u^i} \frac{1}{2}\mathbf{T}_h\,\mathbf{u}_h^T\,dS^i - \int_{S_u^i} \mathbf{T}_h^T\,\mathbf{u}_p\,dS^i + \int_{S_u^i} \mathbf{T}_h^T\,\tilde{\mathbf{u}}\,dS^i + \int_{S_u^i} \mathbf{T}_p^T\,\tilde{\mathbf{u}}\,dS^i \tag{26}$$

$$+ \text{ terms without } \mathbf{u}_h,\ \mathbf{T}_h \text{ and } \tilde{\mathbf{u}}.$$

At this stage of the derivation, the terms in Π_H^i, which are relevant for the variation, are reduced to area integrals over the lateral surfaces of the plate element.

Since the dependence of the fields $\mathbf{u}_h$, $\mathbf{T}_h$, $\mathbf{u}_p$ and $\mathbf{T}_p$ on the thickness coordinate z is known from the representations (4), (10), (11) and the z-dependence of the coupling displacement field can be chosen, the integration of the terms in (26) with respect to the thickness coordinate can be done analytically. In order to carry out the integration in the thickness direction, (26) is rewritten as

$$\Pi_H^i = -\frac{1}{2}\int_{\Gamma^i}\Big[\int_{-h/2}^{h/2} \mathbf{T}_h\,\mathbf{u}_h^T\,dz\Big]\,d\Gamma^i - \int_{\Gamma^i}\Big[\int_{-h/2}^{h/2} \mathbf{T}_h^T\,\mathbf{u}_p\,dz\Big]\,d\Gamma^i \tag{27}$$

$$+ \int_{\Gamma^i}\Big[\int_{-h/2}^{h/2} \mathbf{T}_h^T\,\tilde{\mathbf{u}}\,dz\Big]\,d\Gamma^i + \int_{\Gamma^i}\Big[\int_{-h/2}^{h/2} \mathbf{T}_p^T\,\tilde{\mathbf{u}}\,dz\Big]\,d\Gamma^i$$

$$+ \text{ terms without } \mathbf{u}_h,\ \mathbf{T}_h \text{ and } \tilde{\mathbf{u}},$$

where Γ^i is the boundary of the midsurface of the plate element. The results for the integration in thickness direction are given below (see paragraph 6). For the remaining integrals along the boundary Γ^i, we can get exact results, if we use polynomials in x and y for $\mathbf{u_h}$ and $\mathbf{T_h}$.

5. THE VARIATIONAL FORMULATION IN DISCRETIZED FORM

Writing the discretized fields in the form

$$\mathbf{u_h} = \begin{bmatrix} u_h \\ v_h \\ w_h \end{bmatrix} = \begin{bmatrix} U \\ V \\ W \end{bmatrix} \mathbf{c}, \qquad \mathbf{u_p} = \begin{bmatrix} u_p \\ v_p \\ w_p \end{bmatrix}, \tag{28}$$

$$\mathbf{T_h} = \begin{bmatrix} T_{x_h} \\ T_{y_h} \\ T_{z_h} \end{bmatrix} = \begin{bmatrix} T_x \\ T_y \\ T_z \end{bmatrix} \mathbf{c}, \qquad \mathbf{T_p} = \begin{bmatrix} T_{x_p} \\ T_{y_p} \\ T_{z_p} \end{bmatrix}, \tag{29}$$

$$\tilde{\mathbf{u}} = \begin{bmatrix} \tilde{u} \\ \tilde{v} \\ \tilde{w} \end{bmatrix} = \begin{bmatrix} \tilde{U} \\ \tilde{V} \\ \tilde{W} \end{bmatrix} \mathbf{q}, \tag{30}$$

the functional (27) can be written as

$$\Pi_H^i = -\frac{1}{2}\,\mathbf{c}^T\,\mathbf{H}\,\mathbf{c} + \mathbf{c}^T\,\mathbf{L}\,\mathbf{q} - \mathbf{c}^T\,\mathbf{r_p} + \mathbf{q}^T\,\tilde{\mathbf{r}}_p + \text{ terms without } \mathbf{c} \text{ and } \mathbf{q}, \tag{31}$$

where

$$\mathbf{H} = \int_{\Gamma^i}\int_{-h/2}^{h/2} [\,T_x^T U + T_y^T V + T_z^T W\,]\,dz\,d\Gamma^i \qquad \text{(symmetric)}, \tag{32}$$

$$\mathbf{L} = \int_{\Gamma^i}\int_{-h/2}^{h/2} [\,T_x^T \tilde{U} + T_y^T \tilde{V} + T_z^T \tilde{W}\,]\,dz\,d\Gamma^i, \tag{33}$$

$$\mathbf{r_p} = \int_{\Gamma^i}\int_{-h/2}^{h/2} [\,T_x^T u_p + T_y^T v_p + T_z^T w_p\,]\,dz\,d\Gamma^i, \tag{34}$$

$$\tilde{\mathbf{r}}_p = \begin{bmatrix} \displaystyle\int_{\Gamma^i}\int_{-h/2}^{h/2} \tilde{U}^T\,T_{x_p}\,dz\,d\Gamma^i \\ \displaystyle\int_{\Gamma^i}\int_{-h/2}^{h/2} \tilde{V}^T\,T_{y_p}\,dz\,d\Gamma^i \\ \displaystyle\int_{\Gamma^i}\int_{-h/2}^{h/2} \tilde{W}^T\,T_{z_p}\,dz\,d\Gamma^i \end{bmatrix}. \tag{35}$$

$\mathbf{c}$ is the vector of free parameters, and $\mathbf{q}$ contains the nodal values of the element. From the variation of (31) with respect to $\mathbf{c}^T$ we obtain

$$-\mathbf{H}\,\mathbf{c} + \mathbf{L}\,\mathbf{q} - \mathbf{r}_p = \mathbf{0}, \tag{36}$$

which gives us the relationship

$$\mathbf{c} = \mathbf{H}^{-1}\,\mathbf{L}\,\mathbf{q} - \mathbf{H}^{-1}\,\mathbf{r}_p. \tag{37}$$

The substitution of $\mathbf{c}$ into (31) yields

$$\Pi_H^i = \frac{1}{2}\,\mathbf{q}^T\,\mathbf{L}^T\,\mathbf{H}^{-1}\,\mathbf{L}\,\mathbf{q} - \mathbf{q}^T\,[\,\mathbf{L}^T\,\mathbf{H}^{-1}\,\mathbf{r}_p - \tilde{\mathbf{r}}_p\,] + \text{ terms without } \mathbf{q} \tag{38}$$

so that the element stiffness matrix becomes

$$\mathbf{K} = \mathbf{L}^T\,\mathbf{H}^{-1}\,\mathbf{L} \tag{39}$$

and the element load vector is

$$\mathbf{p} = \mathbf{L}^T\,\mathbf{H}^{-1}\,\mathbf{r}_p - \tilde{\mathbf{r}}_p. \tag{40}$$

6. EXACT INTEGRATION IN THICKNESS DIRECTION

On the lateral surfaces of the plate the direction cosine n_z vanishes so that the tractions reduce to

$$\begin{aligned} T_x &= \sigma_{xx}n_x + \tau_{xy}n_y \qquad \text{on } S_u^i \\ T_y &= \tau_{xy}n_x + \sigma_{yy}n_y \qquad \text{on } S_u^i \\ T_z &= \tau_{xz}n_x + \tau_{yz}n_y \qquad \text{on } S_u^i. \end{aligned} \tag{41}$$

The homogeneous solution parts T_{x_h}, T_{y_h}, T_{z_h}, and the particular parts T_{x_p}, T_{y_p}, T_{z_p} can be simplified accordingly. Using the representation (4), $\mathbf{T}_h$ and $\mathbf{u}_h$ are expressed with the aid of the function G(x,y), which has to satisfy $\Delta\Delta G = 0$. As an example the case of uniform normal loading on the upper face of the plate element is chosen for the illustration of the calculation of an element load vector. For $\mathbf{T}_p$ and $\mathbf{u}_p$ the particular solution given with relationship (10) is used. Since the functional behavior of $\mathbf{T}_h$, $\mathbf{u}_h$, $\mathbf{T}_p$ and $\mathbf{u}_p$ in thickness direction is now given, we only need an expression for the coupling field $\tilde{\mathbf{u}}$ before we can integrate the terms in (27) with respect to z. For the components of the vector $\tilde{\mathbf{u}}$, the following short notation is used: $\tilde{u}(z,s) = \tilde{u}_1(s)\,z + \tilde{u}_2(s)\,z^3$, $\tilde{v}(z,s) = \tilde{v}_1(s)\,z + \tilde{v}_2(s)\,z^3$, $\tilde{w}(z,s) = \tilde{w}_1(s) + \tilde{w}_2(s)\,z^2$. Full expressions for the coefficient functions u_1, u_2, etc., can be taken from a discussion of the element coupling given below (see paragraph 8).

The integration in (27) with respect to the thickness coordinate z can now be carried out analytically and we obtain

$$\int_{-h/2}^{h/2} T_h^T u_h \, dz = \int_{-h/2}^{h/2} [\, T_{x_s} u_h + T_{y_s} v_h + T_{z_s} w_h \,] \, dz = \tag{42}$$

$$\begin{aligned}
&= \Bigg\{ \Bigg[\nu^2 \Big\{ \quad 5h^7 \, (\Delta G_x \, \Delta G_{xx} + \Delta G_y \, \Delta G_{xy}) \\
&\qquad + 168h^5 \, (- G_x \, \Delta G_{xx} - G_y \, \Delta G_{xy} - \Delta G_y \, G_{xy} + \Delta G_x \, G_{yy}) \\
&\qquad + 6720h^3 \, (G_y \, G_{xy} - G_x \, G_{yy}) \Big\} \\
&\quad + \nu \Big\{ \quad 64h^7 \, (\Delta G_x \, \Delta G_{xx} + \Delta G_y \, \Delta G_{xy}) \\
&\qquad + 168h^5 \, (\Delta G_x \, G_{xx} - \Delta G_x \, \Delta G + 8 \Delta G_x \, G_{yy} - 7 \Delta G_{xx} \, G_x - 7 \Delta G_y \, G_{xy} - 7 \Delta G_{xy} \, G_y) \\
&\qquad + 6720h^3 \, (- G_x \, G_{xx} + G_{yy} \, G_x - 2 G_y \, G_{xy} + \Delta G_x \, G) \Big\} \\
&\qquad + 272h^7 \, (\Delta G_x \, \Delta G_{xx} + \Delta G_y \, \Delta G_{xy}) \\
&\qquad + 1344h^5 \, (\Delta G_x \, G_{xx} + \Delta G_{xx} \, G_x + \Delta G_y \, G_{xy} + \Delta G_{xy} \, G_y) \\
&\qquad + 6720h^3 \, (G_x \, G_{xx} + G_y \, G_{xy} - \Delta G_x \, G) \Bigg] \, n_x \\
&\quad + \Bigg[\nu^2 \Big\{ \quad 5h^7 \, (\Delta G_y \, \Delta G_{yy} + \Delta G_x \, \Delta G_{xy}) \\
&\qquad + 168h^5 \, (- G_y \, \Delta G_{yy} - G_x \, \Delta G_{xy} - \Delta G_x \, G_{xy} + \Delta G_y \, G_{xx}) \\
&\qquad + 6720h^3 \, (G_x \, G_{xy} - G_y \, G_{xx}) \Big\} \\
&\quad + \nu \Big\{ \quad 64h^7 \, (\Delta G_y \, \Delta G_{yy} + \Delta G_x \, \Delta G_{xy}) \\
&\qquad + 168h^5 \, (\Delta G_y \, G_{yy} - \Delta G_y \, \Delta G + 8 \Delta G_y \, G_{xx} - 7 \Delta G_{yy} \, G_y - 7 \Delta G_x \, G_{xy} - 7 \Delta G_{xy} \, G_x) \\
&\qquad + 6720h^3 \, (- G_y \, G_{yy} + G_{xx} \, G_y - 2 G_x \, G_{xy} + \Delta G_y \, G) \Big\} \\
&\qquad + 272h^7 \, (\Delta G_y \, \Delta G_{yy} + \Delta G_x \, \Delta G_{xy})
\end{aligned}$$

$$+ 1344h^5 (\Delta G_y G_{yy} + \Delta G_{yy} G_y + \Delta G_x G_{xy} + \Delta G_{xy} G_x)$$

$$+ 6720h^3 (G_y G_{yy} + G_x G_{xy} - \Delta G_y G) \Big] n_y \Big\} / [80640(\nu-1)^2 2\mu]$$

and

$$\int_{-h/2}^{h/2} T_h^T \tilde{u}\, dz = \int_{-h/2}^{h/2} [\, T_{x_s} \tilde{u} + T_{y_s} \tilde{v} + T_{z_s} \tilde{w} \,]\, dz, \tag{43}$$

where

$$\int_{-h/2}^{h/2} T_{x_s} \tilde{u}\, dz = \Bigg\{ \Bigg[\Big[28h^5(\nu + 8)\Delta G_{xx} + 1120h^3(G_{xx} + \nu G_{yy}) \Big] n_x \tag{44}$$

$$+ \Big[28h^5(\nu + 8)\Delta G_{xy} + 1120h^3(1 - \nu) G_{xy} \Big] n_y \Bigg] \tilde{u}_1(s)$$

$$+ \Bigg[\Big[h^7(5\nu + 32)\Delta G_{xx} + 168h^5(G_{xx} + \nu G_{yy}) \Big] n_x$$

$$+ \Big[h^7(5\nu + 32)\Delta G_{xy} + 168h^5(1 - \nu) G_{xy} \Big] n_y \Bigg] \tilde{u}_2(s) \Bigg\} / [13440(\nu-1)],$$

$$\int_{-h/2}^{h/2} T_{y_s} \tilde{v}\, dz = \Bigg\{ \Bigg[\Big[28h^5(\nu + 8)\Delta G_{xy} + 1120h^3(1 - \nu)\, G_{xy} \Big] n_x \tag{45}$$

$$+ \Big[28h^5(\nu + 8)\Delta G_{yy} + 1120h^3(G_{yy} + \nu G_{xx}) \Big] n_y \Bigg] \tilde{v}_1(s)$$

$$+ \Bigg[\Big[h^7(5\nu + 32)\Delta G_{xy} + 168h^5(1 - \nu)\, G_{xy} \Big] n_x$$

$$+ \Big[h^7(5\nu + 32)\Delta G_{yy} + 168h^5(G_{yy} - \nu G_{xy}) \Big] n_y \Bigg] \tilde{v}_2(s) \Bigg\} / [13440(\nu-1)],$$

$$\int_{-h/2}^{h/2} T_{z_s} \tilde{w}\, dz = \Bigg\{ \Big[20h^3\, \Delta G_x\, n_x + 20h^3\, \Delta G_y\, n_y \Big] \tilde{w}_1(s) \tag{46}$$

$$+ \Big[h^5\, \Delta G_x\, n_x + h^5\, \Delta G_y\, n_y \Big] \tilde{w}_2(s) \Bigg\} / [240(\nu-1)].$$

The remaining terms in (27) contain the particular solution vectors $\mathbf{u_p}$ and $\mathbf{T_p}$. The integration with respect to z is explicitly carried out for the example of a constant normal load p on the upper face of the plate element. Using the particular solution functions given with relationships (10) and noting that $\mathbf{T_h^T u_p} = T_{x_h} u_p + T_{y_h} v_p + T_{z_h} w_p$ and $\mathbf{T_p^T \tilde{u}} = T_{x_p} \tilde{u} + T_{y_p} \tilde{v} + T_{z_p} \tilde{w}$ we obtain

$$\int_{-h/2}^{h/2} T_{x_h} u_p \, dz = p \Big\{ \Big[\Big[\big[21h^2(\nu^2 + 7\nu - 8)\Delta G_{xx} + 840\nu(\nu - 1)G_{yy} + 840(\nu - 1)G_{xx} \big] n_x + \big[21h^2(\nu^2 + 7\nu - 8)\Delta G_{xy} - 840(\nu - 1)^2 G_{xy} \big] n_y \Big] x (x^2 + y^2) + \Big[\big[h^4(16\nu^2 + 104\nu - 272)\Delta G_{xx} + 672h^2\nu(\nu - 2)G_{yy} + 672h^2(\nu - 2)G_{xx} \big] n_x + \big[h^4(16\nu^2 + 104\nu - 272)\Delta G_{xy} + 672h^2\nu(-\nu^2 + 3\nu - 2)G_{xy} \big] n_y \Big] x \Big\} / [2\mu 13440(\nu - 1)] \tag{47}$$

$$\int_{-h/2}^{h/2} T_{y_h} v_p \, dz = p \Big\{ \Big[\Big[\big[21h^2(\nu^2 + 7\nu - 8)\Delta G_{xy} - 840(\nu - 1)^2 G_{xy} \big] n_x + \big[21h^2(\nu^2 + 7\nu - 8)\Delta G_{yy} + 840\nu(\nu - 1)G_{xx} + 840(\nu - 1)G_{yy} \big] n_y \Big] y (x^2 + y^2) + \Big[\big[h^4(16\nu^2 + 104\nu - 272)\Delta G_{xy} + 672h^2\nu(-\nu^2 + 3\nu - 2)G_{xy} \big] n_x + \big[h^4(16\nu^2 + 104\nu - 272)\Delta G_{yy} + 672h^2\nu(\nu - 2)G_{xx} + 672h^2(\nu - 2)G_{yy} \big] n_y \Big] y \Big\} / [2\mu 13440(\nu - 1)] \tag{48}$$

$$\int_{-h/2}^{h/2} T_{z_h} w_p \, dz = -p \big[\Delta G_x n_x + \Delta G_y n_y \big] \big[70(\nu - 1)(x^2 + y^2)^2 + 112h^2\nu(x^2 + y^2) - 13h^4(1 + \nu) \big] / [2\mu 4480(\nu - 1)] \tag{49}$$

and

$$\int_{-h/2}^{h/2} \tilde{u}\, T_{x_p}\, dz = -p \Big\{ \tilde{u}_1(s) \Big[\Big[112h^2(2+\nu) + 140(3+\nu)x^2 + 140(1+3\nu)y^2 \Big] n_x + \Big[280(1-\nu)xy \Big] n_y \Big] + \tilde{u}_2(s) \Big[\Big[16h^4(2+\nu) + 21h^2(3+\nu)x^2 + 21h^2(1+3\nu)y^2 \Big] n_x + \Big[42h^2(1-\nu)xy \Big] n_y \Big] \Big\} / 2240 \quad (50)$$

$$\int_{-h/2}^{h/2} \tilde{v}\, T_{y_p}\, dz = -p \Big\{ \tilde{v}_1(s) \Big[\Big[280(1-\nu)xy \Big] n_x + \Big[112h^2(2+\nu) + 140(1+3\nu)x^2 + 140(3+\nu)y^2 \Big] n_y \Big] + \tilde{v}_2(s) \Big[\Big[42h^2(1-\nu)xy \Big] n_x + \Big[16h^4(2+\nu) + 21h^2(1+3\nu)x^2 + 21h^2(3+\nu)y^2 \Big] n_y \Big] \Big\} / 2240 \quad (51)$$

$$\int_{-h/2}^{h/2} \tilde{w}\, T_{z_p}\, dz = -p \Big\{ \tilde{w}_1(s) \Big[20(x\, n_x + y\, n_y) \Big] + \tilde{w}_2(s) \Big[h^2(x\, n_x + y\, n_y) \Big] \Big\} / 40. \quad (52)$$

7. SYSTEMATIC CONSTRUCTION OF LINEAR INDEPENDENT DISPLACEMENT AND STRESS FUNCTIONS

In order to construct a set of linearly independent displacement and stress functions from the homogeneous solution part (4), a complex representation of the real function G(x,y) is used. The biharmonic function G(x,y) can be expressed with the aid of two complex functions $\Phi(\zeta)$ and $\chi(\zeta)$ in the form

$$G(x,y) = \mathrm{Re}[\, \bar{\zeta}\, \Phi + \chi \,], \quad (53)$$

where $\zeta = x + iy$. The partial derivatives of G(x,y) in the displacement and stress representation (4) can be written in terms of the complex functions in the following form:

$$
\begin{aligned}
G_x &= \mathrm{Re}[\, \Phi + \zeta \overline{\Phi'} + \overline{\chi'} \,], \\
G_y &= \mathrm{Im}[\, \Phi + \zeta \overline{\Phi'} + \overline{\chi'} \,], \\
G_{xx} &= \mathrm{Re}[\, \Phi' + \overline{\Phi'} + \zeta \overline{\Phi''} + \overline{\chi''} \,], \\
G_{yy} &= \mathrm{Re}[\, \Phi' + \overline{\Phi'} - \zeta \overline{\Phi''} - \overline{\chi''} \,], \\
G_{xy} &= \mathrm{Im}[\, \zeta \overline{\Phi''} + \overline{\chi''} \,], \\
\Delta G &= 4\, \mathrm{Re}[\, \Phi' \,], \\
\frac{\partial}{\partial x}\Delta G &= 4\, \mathrm{Re}[\, \Phi'' \,], \\
\frac{\partial}{\partial y}\Delta G &= -4\, \mathrm{Im}[\, \Phi'' \,], \\
\frac{\partial^2}{\partial x^2}\Delta G &= 4\, \mathrm{Re}[\, \Phi''' \,], \\
\frac{\partial^2}{\partial y^2}\Delta G &= -4\, \mathrm{Re}[\, \Phi''' \,], \\
\frac{\partial^2}{\partial x \partial y}\Delta G &= -4\, \mathrm{Im}[\, \Phi''' \,].
\end{aligned}
\tag{54}
$$

A simple choice for the complex functions is

$$\Phi(\zeta) = \sum_{j=1}^{N} a_j \left(\frac{\zeta}{c}\right)^j \tag{55}$$

$$\chi(\zeta) = \sum_{j=2}^{N} b_j \left(\frac{\zeta}{c}\right)^j, \tag{56}$$

where $\zeta = x + iy$, $a_1 = \alpha_1$, $a_j = \alpha_j + \beta_j$, $b_j = \gamma_j + \delta_j$ and c is a normalization factor defined below (see equation (60)). The terms with the coefficients a_0, b_0 , b_1 and β_1 are excluded from the series (55), (56), since they either do not contribute to the displacements and stresses or they lead to rigid body terms.

The complex powers can be easily computed using polar coordinates $r = \sqrt{x^2 + y^2}$ and $\theta = \arctan(y/x)$; the resultant equation is expressed as follows:

$$\left(\frac{\zeta}{c}\right)^j = \left(\frac{r}{c}\right)^j \cos j\theta + i \left(\frac{r}{c}\right)^j \sin j\theta. \tag{57}$$

The real and imaginary parts of $(\zeta/c)^j$ can be of course also written as polynomials in x and y, giving the harmonic polynomials x/c, y/c, $(x^2-y^2)/c^2$, xy/c^2, $x(x^2-3y^2)/c^3$, $y(3x^2-y^2)/c^3$, etc.

The number of displacement function terms obtained from (55) and (56) is $NFT=4N-3$. The upper summation limit N in (55) and (56) is chosen such that $NFT \geq NDF-3$, where (NDF-3) is the number of degrees of freedom of the element minus the number of rigid body modes. For the element considered in this paper $NDF=24$, and N is chosen as $N=6$.

The real coefficients α_j, β_j, γ_j, δ_j can be arranged into one vector of free parameters $\mathbf{c}$ in the form $\mathbf{c}^T = [\, \alpha^T, \beta^T, \gamma^T, \delta^T \,]$.

For a quadrilateral element the origin of the local coordinate system is set at the center of the element. The global coordinates (X_0, Y_0) of the element center are

$$X_0 = [\, (X_3 - X_1)X_2Y_4 + (X_2 - X_4)X_1Y_3 + (X_1 - X_3)X_4Y_2 + (X_4 - X_2)X_3Y_1 \,]/d, \tag{58}$$

$$Y_0 = [\, (X_2 - X_1)Y_3Y_4 + (X_3 - X_2)Y_1Y_4 + (X_1 - X_4)Y_2Y_3 + (X_4 - X_3)Y_1Y_2 \,]/d,$$

where

$$d = (X_3 - X_1)(Y_4 - Y_2) + (X_4 - X_2)(Y_1 - Y_3), \tag{59}$$

and the X_i, Y_i $(i=1,2,3,4)$ define the corner node points of the quadrilateral element in global coordinates. For the calculations of the examples in this paper, the normalization factor c was chosen as

$$c = \frac{1}{4}(r_1 + r_2 + r_3 + r_4), \tag{60}$$

where $r_i = \sqrt{x_i^2 + y_i^2}$ $(i=1,2,3,4)$. The local nodal coordinates x_i, y_i are measured from the center of the element.

8. CONSTRUCTION OF THE BOUNDARY DISPLACEMENT FIELD $\bar{u}$

With the choice of the independently assumed boundary displacement field $\bar{\mathbf{u}} = [\, \bar{u}, \bar{v}, \bar{w} \,]^T$ we define the nodal values of the plate element. In order to get a coupling displacement field $\tilde{u}$, which is not too complicated, and to keep the number of unknown nodal values low, the following simplified boundary displacements are chosen:

$$\tilde{u} = -z \frac{\partial}{\partial x}\bar{w}(s) - \frac{1}{4(1-\nu)} [\, h^2 z - 2(2-\nu)\frac{z^3}{3} \,] \bar{q}_x(s),$$

$$\bar{v} = -z \frac{\partial}{\partial y}\bar{w}(s) - \frac{1}{4(1-\nu)} [\, h^2 z - 2(2-\nu)\frac{z^3}{3} \,] \bar{q}_y(s), \tag{61}$$

$$\bar{w} = \bar{w}(s),$$

where s is a boundary coordinate on Γ^i.

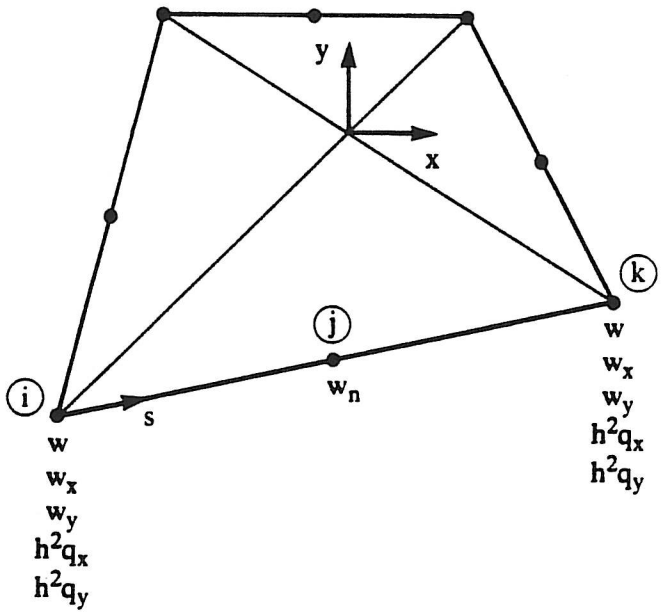

Figure 1: Quadrilateral plate bending element

The quadrilateral plate bending element proposed in this paper has 24 degrees of freedom (Figure 1). At the corner nodes the unknowns are chosen to be w, w_x, w_y, (h^2q_x), (h^2q_y). The values q_x and q_y characterize the magnitude of warping and are proportional to the shear forces Q_x and Q_y. At each midside node the unknown is w_n.

The transverse displacement of the middle surface along the element boundary is chosen as

$$\bar{w}(s) = N_1(s)\, w_i + N_2(s) \left(\frac{\partial w}{\partial s}\right)_i + N_3(s)\, w_k + N_4(s) \left(\frac{\partial w}{\partial s}\right)_k, \tag{62}$$

where

$$N_1(s) = 1 - 3\xi^2 + 2\xi^3,$$

$$N_2(s) = l\,[\, \xi - 2\xi^2 + \xi^3 \,],$$

$$N_3(s) = 3\xi^2 - 2\xi^3, \tag{63}$$

$$N_4(s) = l\,[\,\xi^3 - \xi^2\,],$$

and

$$\xi = \frac{s}{l}. \tag{64}$$

Note that l is the distance between node i and node k (Figure 1). In addition to (62), the normal derivative of the boundary deflection is chosen in the form

$$\frac{\partial \tilde{w}(s)}{\partial n} = N_5(s)\left[\frac{\partial w}{\partial n}\right]_i + N_6(s)\left[\frac{\partial w}{\partial n}\right]_j + N_7(s)\left[\frac{\partial w}{\partial n}\right]_k, \tag{65}$$

where

$$\begin{aligned} N_5(s) &= 1 - 3\xi + 2\xi^2, \\ N_6(s) &= 4\xi - 4\xi^2, \\ N_7(s) &= 2\xi^2 - \xi. \end{aligned} \tag{66}$$

From (62) the derivative of $\tilde{w}(s)$ with respect to s can be calculated as

$$\frac{\partial \tilde{w}(s)}{\partial s} = N_1'(s)\,w_i + N_2'(s)\left[\frac{\partial w}{\partial s}\right]_i + N_3'(s)\,w_k + N_4'(s)\left[\frac{\partial w}{\partial s}\right]_k, \tag{67}$$

where

$$\begin{aligned} N_1'(s) &= \frac{1}{l}\left(-6\xi + 6\xi^2\right), \\ N_2'(s) &= -1 - 4\xi + 3\xi^2, \\ N_3'(s) &= \frac{1}{l}\left(6\xi - 6\xi^2\right), \\ N_4'(s) &= 3\xi^2 - 2\xi. \end{aligned} \tag{68}$$

The node values w_s and w_n can be substituted by the node values w_x and w_y using the relationship

$$\begin{bmatrix} \frac{\partial w}{\partial n} \\ \frac{\partial w}{\partial s} \end{bmatrix} = \begin{bmatrix} n_x & n_y \\ -n_y & n_x \end{bmatrix} \begin{bmatrix} \frac{\partial w}{\partial x} \\ \frac{\partial w}{\partial y} \end{bmatrix}, \tag{69}$$

where

$$\begin{aligned} n_x &= \frac{y_k - y_i}{l} \\ n_y &= -\frac{x_k - x_i}{l} \end{aligned} \tag{70}$$

and

$$l = \sqrt{(x_k - x_i)^2 + (y_k - y_i)^2}. \tag{71}$$

For the assumed boundary displacements $\tilde{u}$ and $\tilde{v}$ we need the partial derivatives $\tilde{w}_x$ and $\tilde{w}_y$, which can be obtained from the relationship

$$\begin{bmatrix} \frac{\partial w}{\partial x} \\ \frac{\partial w}{\partial y} \end{bmatrix} = \begin{bmatrix} n_x & -n_y \\ n_y & n_x \end{bmatrix} \begin{bmatrix} \frac{\partial w}{\partial n} \\ \frac{\partial w}{\partial s} \end{bmatrix}. \tag{72}$$

Using (65)-(72) we obtain

$$\frac{\partial \tilde{w}(s)}{\partial x} = - N_1' n_y w_i + \left[N_5 n_x^2 + N_2' n_y^2 \right] \left(\frac{\partial w}{\partial x} \right)_i + \left[N_5 - N_2' \right] n_x n_y \left(\frac{\partial w}{\partial y} \right)_i + N_6 n_x \left(\frac{\partial w}{\partial n} \right)_j$$

$$- N_3' n_y w_k + \left[N_7 n_x^2 + N_4' n_y^2 \right] \left(\frac{\partial w}{\partial x} \right)_k + \left[N_7 - N_4' \right] n_x n_y \left(\frac{\partial w}{\partial y} \right)_k, \tag{73}$$

$$\frac{\partial \tilde{w}(s)}{\partial y} = N_1' n_x w_i + \left[N_5 - N_2' \right] n_x n_y \left(\frac{\partial w}{\partial x} \right)_i + \left[N_5 n_y^2 + N_2' n_x^2 \right] \left(\frac{\partial w}{\partial y} \right)_i + N_6 n_y \left(\frac{\partial w}{\partial n} \right)_j$$

$$+ N_3' n_x w_k + \left[N_7 - N_4' \right] n_x n_y \left(\frac{\partial w}{\partial x} \right)_k + \left[N_7 n_y^2 + N_4' n_x^2 \right] \left(\frac{\partial w}{\partial y} \right)_k. \tag{74}$$

The boundary functions for $\tilde{q}_x(s)$ and $\tilde{q}_y(s)$, which have the task of coupling the warping terms along the element boundary and which are proportional to the shear forces Q_x and Q_y, are assumed in the form

$$\tilde{q}_x(s) = N_8(s) (q_x)_i + N_9(s) (q_x)_k,$$

$$\tilde{q}_y(s) = N_8(s) (q_y)_i + N_9(s) (q_y)_k, \tag{75}$$

where

$$N_8(s) = 1 - \xi,$$

$$N_9(s) = \xi. \tag{76}$$

It is important to note that in the element stiffness matrix the diagonal terms associated to the nodal values q_x and q_y become much smaller than the other diagonal terms when the plate thickness becomes small in comparison to the other dimensions. In order to get good transverse shear results for thick and thin plates, scaling of the element matrix has been used. Instead of solving for q_x and q_y, the unknowns are chosen to be $(h^2 q_x)$ and $(h^2 q_y)$. This means that the according rows and columns in the element stiffness matrix have to be divided by h^2 giving a

diagonal term which is divided by h^4. The associated values in the element load vector are also divided by h^2.

9. SOME REMARKS

The presented plate element can be considered as a 3-dimensional continuum element. Due to the properties of the element trial functions, which a priori satisfy the equilibrium equations and the stress boundary conditions on the upper and lower faces of the plate, the element stiffness matrix and the element load vector can be obtained through the numerical evaluation of line integrals along the boundary of the element midsurface. However, exact integration results can be obtained by using Gauss-integration formulas, since the trial functions for G(x,y), which are generated with the aid of the complex functions (55) and (56), are polynomials in x and y. Formulas of different orders can be used for the matrices **H**, **L** and the vectors $\mathbf{r}_p$ and $\tilde{\mathbf{r}}_p$, since each of them contain polynomials of different orders. The symmetric matrix **H** requires the highest order of Gauss-integration in order to get exact stiffness coefficients. A Gauss-integration formula of the order n=7 was used for the examples.

An alternative to the use of Gauss-integration is to evaluate the boundary integrals analytically once and for ever in terms of the nodal element coordinates. This can be done automatically by using a symbolic manipulation program such as MACSYMA [69,70]. Using MACSYMA it is possible to convert the obtained algebraic expressions directly into FORTRAN-statements so that typing of the according FORTRAN-statements becomes unnecessary.

The stiffness matrix of the proposed 24 degree of freedom hybrid plate bending element has 3 eigenvalues equal to zero.

10. NUMERICAL EXAMPLES

Simply supported plate

One quarter of a rectangular simply supported plate, with a constant normal load p=1 on the upper plate face, was analyzed using the proposed 24-degree of freedom plate element. The numerical results are compared with the exact 3-dimensional solution, which is taken from reference [23]. The exact solution is given in form of an infinite series. The values for the exact solution in the tables are computed for the upper summation limits m=21 and n=21. The stresses σ_{xx}, σ_{yy}, and τ_{xy} are taken at the upper face of the plate, whereas the shear stresses τ_{xz}, τ_{yz} and the deflection w is calculated for the midsurface of the plate.

The boundary conditions for the 3-dimensional plate model are

$$w = v = \sigma_{xx} = 0 \quad \text{on } x = 0 \text{ and } x = a \tag{76}$$

and

$$w = u = \sigma_{yy} = 0 \quad \text{on } y = 0 \text{ and } y = b. \tag{77}$$

The boundary conditions for the finite element model are

$$\begin{aligned} w = w_y = q_y = 0 \quad &\text{on } x = 0 \\ w = w_x = q_x = 0 \quad &\text{on } y = 0 \\ w_x = q_x = 0 \quad &\text{on } x = a/2 \\ w_y = q_y = 0 \quad &\text{on } y = b/2. \end{aligned} \tag{78}$$

In Table I, the deflection at the center of the plate is given for different discretizations and compared to the exact 3-dimensional solution. For every mesh, the numerical calculated value for the energy is listed in Table I as well.

For a mesh with 64 elements, very good stress and displacement results have been obtained (see Tables II, III). No percentage errors are given in the tables when the value for the exact stress is zero.

Along the plate boundary y=0, the transverse shear τ_{yz} has been calculated for z=0 at the element corner nodes. For those boundary nodes, where two elements are coupled, two shear values are given in Table III, and the error is calculated from the meanvalues of the shear stresses of the adjacent elements. In Table III we see a good agreement of the transverse shear

distribution in comparison with the exact 3-dimensional solution.

Table I: Deflection w at the center of a simply supported rectangular plate (a=6, b=4, h=0.2, E=1, ν=0.3, uniform load p=1) for different discretizations.

number of elements	energy	w (numerical)	w exact [23]	error %
1	5994.1	2609.7	2721.4	4.1
4	7026.5	2750.4	2721.4	1.1
16	7051.2	2748.2	2721.4	0.98
64	6964.7	2730.03	2721.4	0.3

Table II: Results at the center of a simply supported rectangular plate (a=6, b=4, h=0.2, E=1, ν=0.3, uniform load p=1) for a discretization with 64 elements.

	numerical 64 elements	exact (3-D) [23]	error %
σ_{xx}	-120.3	-120.0	0.2
σ_{yy}	-195.9	-195.1	0.4
τ_{xy}	-0.0385	0.0	
τ_{xz}	-0.0556	0.0	
τ_{yz}	0.0496	0.0	
w	2730.03	2721.4	0.3

Table III: Transverse shear stress τ_{yz} for a simply supported rectangular plate (a=6, b=4, h=0.2, E=1, ν=0.3, uniform load p=1, 64 elements) along the boundary y=0.

τ_{yz} on y=0, z=0			
x	numerical	exact [23]	error %
0.0	−0.0656	0.0	
0.75	7.712 | 7.554	7.564	0.9
1.5	10.72 | 10.63	10.59	0.8
2.25	12.11 | 12.03	11.99	0.7
3.0	12.33	12.30	0.2

In the next test the influence of the thickness h on the accuracy of the results has been studied. The results for a coarse mesh of 4x4 elements are listed in Tables IV and V. Good results are obtained for both thick and thin plates.

Table IV: Deflection at the center of a simply supported rectangular plate (a=6, b=4, E=1, ν=0.3, uniform load p=1, 16 elements) for different thickness values h.

	thickness h	numerical solution	exact solution [23]	error %
w	1	$2.5381 * 10^1$	$2.6016 * 10^1$	2.4
w	0.8	$4.7134 * 10^1$	$4.7721 * 10^1$	1.2
w	0.6	$1.0708 * 10^2$	$1.0738 * 10^2$	0.3
w	0.4	$3.5000 * 10^2$	$3.4853 * 10^2$	0.4
w	0.2	$2.7482 * 10^3$	$2.7214 * 10^3$	0.98
w	0.1	$2.1910 * 10^4$	$2.1637 * 10^4$	1.3
w	0.01	$2.1890 * 10^7$	$2.1593 * 10^7$	1.4
w	0.001	$2.1891 * 10^{10}$	$2.1593 * 10^{10}$	1.4

Table V: Normal stresses at the center of a simply supported rectangular plate (a=6, b=4, E=1, ν=0.3, uniform load p=1, 16 elements) for different thickness values h.

	thickness h	numerical solution	exact solution [23]	error %
σ_{yy}	1.0	−7.910	−8.076	2.1
σ_{yy}	0.8	$-1.234 * 10^1$	$-1.246 * 10^1$	0.9
σ_{yy}	0.6	$-2.190 * 10^1$	$-2.193 * 10^1$	0.1
σ_{yy}	0.4	$-4.922 * 10^1$	$-4.898 * 10^1$	0.5
σ_{yy}	0.2	$-1.973 * 10^2$	$-1.951 * 10^2$	1.2
σ_{yy}	0.1	$-7.930 * 10^2$	$-7.795 * 10^2$	1.7
σ_{yy}	0.01	$-7.971 * 10^4$	$-7.792 * 10^4$	2.3
σ_{yy}	0.001	$-7.972 * 10^6$	$-7.792 * 10^6$	2.3
σ_{xx}	1.0	−4.761	−5.153	7.6
σ_{xx}	0.8	−7.499	−7.845	4.4
σ_{xx}	0.6	$-1.343 * 10^1$	$-1.366 * 10^1$	1.7
σ_{xx}	0.4	$-3.039 * 10^1$	$-3.027 * 10^1$	0.4
σ_{xx}	0.2	$-1.215 * 10^2$	$-1.200 * 10^2$	1.2
σ_{xx}	0.1	$-4.821 * 10^2$	$-4.790 * 10^2$	0.7
σ_{xx}	0.01	$-4.775 * 10^4$	$-4.786 * 10^4$	0.2
σ_{xx}	0.001	$-4.774 * 10^6$	$-4.786 * 10^6$	0.3

It should be noted that the errors for the thick plate examples, with h=1 and h=0.8, are bigger than for the other results in Table V, because for these cases the membrane stresses are already recognizable. The normal stresses at the upper and lower faces of the plate have not the same absolute value for these cases. From the exact solution representation [23] we get for the plate with the thickness h=1.0 the following results: σ_{yy}= −8.076 for z= −h/2, σ_{yy}=7.958 for z=h/2, and σ_{xx}= −5.153 for z= −h/2, σ_{xx}=4.878 for z=h/2. For the plate with the thickness h=0.8 the exact solutions are: σ_{yy}= −1.246 for z= −h/2, σ_{yy}=1.234 for z=h/2,and σ_{xx}= −7.845 for

$z=-h/2$, $\sigma_{xx}=7.57$ for $z=h/2$. The stress results of the proposed element, which accounts only for bending (so that the normal stresses at the upper and lower plate faces have the same absolute value), appear to be closer to the exact 3-dimensional solution at the lower face of the plate.

Clamped plate

For a clamped square plate, the convergence of the numerical solution has been studied. For different discretizations, the energy and the maximum displacement have been calculated (Table VI). The comparison values for w are calculated from an exact thin plate solution [71]. It should be noted that the element does not lock for a discretization with one element and only one active degree of freedom (D.O.F.) left in the system.

Table VI: Deflection w at the center of a clamped square plate ($a=b=5$, $h=0.01$, $E=10.92 * 10^6$, $\nu=0.3$, uniform load $p=1$) for different discretizations.

number of elements	D.O.F. (active)	energy	w (numerical)	w exact [71]	error %
1	1	83.01	13.28	12.64	5.1
4	16	96.92	12.66	12.64	0.2
16	88	97.280	12.65	12.64	0.08
64	400	97.286	12.65	12.64	0.08

Mesh sensitivity test

In order to test the sentivity of the numerical results to the element shapes in the mesh, one quarter of a clamped square plate has been analyzed with different mesh forms. For a coarse mesh of 4 elements, the shape of the elements has been distorted with the aid of the parameter Δ (Figure 2). No severe influence of the mesh distortion on the results can be observed from Table VII. Even when two elements take almost the shape of a triangle (which means that the discretized system practically looses degrees of freedom) the results for the chosen coarse discretization remain acceptable.

Table VII: Test on mesh sensitivity for a clamped square plate (a=b=10, h=0.01, $E=10.92 * 10^6$, $\nu=0.3$, uniform load p=1, 4 elements) for different mesh distortion parameters Δ (Figure 2).

Δ	energy	center displacement w (numerical)	center displacement w (exact [71])	error %
-2.49	86.49	11.76	12.64	6.9
-2.0	90.86	12.09	12.64	4.4
-1.5	93.35	12.28	12.64	2.8
-1.0	95.08	12.43	12.64	1.7
-0.5	96.31	12.56	12.64	0.6
0.	96.92	12.66	12.64	0.2
0.1	96.93	12.68	12.64	0.3
0.2	96.91	12.69	12.64	0.4
0.5	96.63	12.72	12.64	0.6
1.0	95.55	12.74	12.64	0.8
1.5	93.51	12.7	12.64	0.5
2.0	89.88	12.5	12.64	1.1
2.4	86.10	12.23	12.64	3.2
2.49	85.13	12.15	12.64	3.9

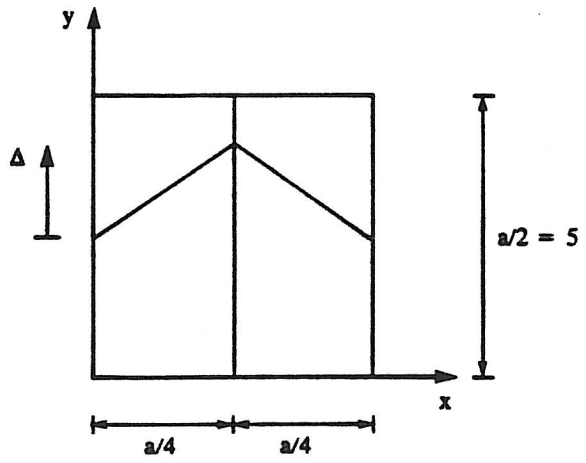

Figure 2: Mesh distortion for clamped square plate (Due to symmetry with respect to x=a/2 and y=a/2 only one quadrant is discretized).

CONCLUSIONS

A simplified plate theory for the inclusion of warping and transverse shear deformations has been discussed, and on its basis a 24-degree of freedom plate element has been derived. The stress and displacement fields used for this element satisfy a priori the 3-dimensional Navier-equations and equilibrium equations, respectively. High accuracy for both displacements and stresses can be achieved using rather coarse meshes. Moreover, transverse shear stresses can be calculated accurately for thick and thin plates.

For the discussed simplified plate theory, a complex function representation was used to obtain compatible displacements and stresses so that the boundary element algorithm proposed in references [72,73] is also applicable to the present plate formulation for the inclusion of warping.

ACKNOWLEDGEMENT

I would like to thank Professor R.L. Taylor for helpful discussions and his encouraging support of this work. Moreover, I gratefully acknowledge the support from the DFG (Deutsche Forschungsgemeinschaft).

REFERENCES

[1] D.N. Arnold and R.S. Falk, " A uniformly accurate finite element method for Mindlin-Reissner plate", IMA Preprint Series No. 307, Institute for Mathematics and its Applications, University of Minnesota, April 1987.

[2] K.J. Bathe and E.N. Dvorkin, "A four node plate bending element based on Mindlin/Reissner plate theory and mixed interpolation", Int. J. Numer. Meth. Eng., 21, 367 - 383, (1985).

[3] J.L. Batoz, "An explicit formulation for an efficient triangular plate bending element", Int. J. Numer. Meth. Eng., 18, 1077 - 1089, (1982).

[4] J.L. Batoz, K.J. Bathe and L.W. Ho, "A study of three node triangular plate bending elements", Int. J. Numer. Meth. Eng., 15, 1771 - 1812, (1980).

[5] J.L. Batoz and M. Ben Tohar, "Evaluation of a new quadrilateral thin plate bending element", Int. J. Numer. Meth. Eng., 18, 1655 - 1677, (1982).

[6] K.J. Bathe, E.N. Dvorkin and L.W. Ho, "On discrete Kirchhoff and isoparametric shell elements for nonlinear analysis - an assessment", J. Comp. Struct., 16, 89 - 98, (1982).

[7] R.D. Cook, D.S. Malkus and M.E. Plesha, "Concepts and Applications of Finite Element Analysis", Wiley & Sons, New York, 1989.

[8] M.A. Crisfield, "A four-noded thin-plate bending element using shear constrains - a modified version of Lyon's element", Comp. Meth. Appl. Mech. Eng., 38, 93 - 120, (1983).

[9] E.N. Dvorkin and K.J. Bathe, "A continuum mechanics based four node shell element for general non-linear analysis", Eng. Comp., 1, 77 - 88, (1984).

[10] E. Hinton and H.C. Huang, "A family of quadrilateral Mindlin plate elements with substitute shear strain fields", Comp. and Struct., 23, 409 - 431, (1986).

[11] H.C. Huang and E. Hinton, "A nine node Lagrangian Mindlin element with enhanced shear interpolation", Eng. Comp., 1, 369 - 380, (1984).

[12] T.J.R. Hughes, "The Finite Element Method", Prentice-Hall, Englewood Cliffs, N.J., 1987.

[13] T.J.R. Hughes, R.L. Taylor and W. Kanoknukulchai, "A simple and efficient element for plate bending", Int. J. Numer. Meth. Eng., 11, 1529 - 1543, (1977).

[14] T.J.R. Hughes and T.E. Tezduyar, "Finite elements based upon Mindlin plate theory with particular reference to the four node bilinear isoparametric element", J. Appl. Mech., 46, 587 - 596, (1981).

[15] Hughes, T.J.R. and Hinton, E. (eds.), Finite Element Methods for Plate and Shell Structures, Volumes 1 and 2, Pineridge Press, Swansea, 1986

[16] J. Jirousek, and L. Guex, "The hybrid-Trefftz finite element model and its application to plate bending", Int. J. Numer. Methods Eng., 23, 651 - 693, (1986).

[17] J. Jirousek and A. Venkatesh, "Implementation of curvilinear geometry into p-version HT plate elements", Int. J. Numer. Meth. Eng., 28, 431 - 443, (1989).

[18] J. Jirousek, "Hybrid-Trefftz plate bending elements with p-method capabilities", Int. J. Numer. Meth. Eng., 24, 1367 - 1393, (1987).

[19] S.S. Murthy and R.H. Gallagher, "A triangular thin-shell finite element based on discrete Kirchhoff theory", Comp. Meth. Appl. Mech. Eng., 54, 197 - 222, (1986).

[20] J.C. Nagtegaal and S. Nakazawa, "On the construction of optimal Mindlin type plate and shell elements", in: Finite Element Methods for Plate and Shell Structures, Volume 1: Element Technology, (T.J.R. Hughes and E. Hinton, eds.), Pineridge Press, 1986.

[21] P. Papadopoulos and R.L. Taylor, "A triangular element based on Reissner-Mindlin plate theory", Report No. UCB/SEMM-89/19, Department of Civil Engineering, University of California at Berkeley, 1989.

[22] T.H.H. Pian, D. Kang and C. Wang, "Hybrid plate elements based on balanced stresses and displacements", in: State-of-the-Art on Finite Element Methods in Plate and Shell Structures, Vol. 1, Element Technology (Edited by T.J.R. Hughes and E. Hinton), pp. 244 - 265, Pineridge Press, Swansea (1986).

[23] R. Piltner, "The application of a complex 3-dimensional elasticity solution representation for the analysis of a thick rectangular plate", Acta Mechanica, 75, 77 - 91, (1988).

[24] E.D.L Pugh, E. Hinton and O.C. Zienkiewicz, "A study of quadrilateral plate bending elements with reduced integration", Int. J. Numer. Meth. Eng., 12, 1059 - 1079, (1978).

[25] A. Razzaque, "Program for triangular bending elements with derivative smoothing", Int. J. Numer. Meth. Eng., 6, 333 - 345, (1973).

[26] J.C. Simo and M.S. Rifai, "A class of mixed assumed strain methods and the method of incompatible modes", Int. J. Numer. Meth. Eng., 29, 1595 - 1638, (1990).

[27] R.L. Spilker, "Invariant 8-node hybrid-stress elements for thin and moderately thick plates", Int. J. Numer. Meth. Eng., 18, 1153 - 1178, (1982).

[28] R.L. Spilker and T. Belytsckko, "Bilinear Mindlin plate elements", Chapter 6, p. 117 - 136, in: Hybrid and Mixed Finite Element Methods, (Eds.: S.N. Atluri, R.H. Gallagher and O.C. Zienkiewicz), Wiley & Sons, New York, 1983.

[29] H. Stolarski and M.Y.M. Chiang, "Thin plate elements with relaxed Kirchhoff constraints", Int. J. Numer. Meth. Eng., 26, 913 - 934, (1988).

[30] R.L. Taylor and J.C. Simo, "Bending and membrane elements for analysis of thick and thin shells", in: Proceedings of the NUMETA 85 Conference, (Eds.: J. Middleton/ G.N.Pande), Vol. 2, 587 - 591, A.A Balkema, Rotterdam/Boston, (1985).

[31] P. Tong, "A family of hybrid plate elements", Int. J. Numer. Meth. Eng., 18, 1455 - 1468, (1982).

[32] S.L. Weissman and R.L. Taylor, "Resultant fields for mixed plate bending elements", Comp. Meth. Appl. Mech. Eng., 79, 321 - 355, (1990).

[33] W. Wunderlich, "Mixed models for plates and shells: priciples - elements - examples", Chapter 11, p. 215 - 241, in: Hybrid and Mixed Finite Element Methods, (Eds.: S.N. Atluri, R.H. Gallagher and O.C. Zienkiewicz), Wiley & Sons, New York, 1983.

[34] F.-G. Yuan and R.E. Miller, "A cubic triangular finite element for flat plates with shear", Int. J. Numer. Meth. Eng., 28, 109 - 126, (1989).

[35] O.C. Zienkiewicz and D. Lefebvre, "Three field mixed approximation and the plate bending problem", Comm. Appl. Numer. Meth., 3, 301 - 309, (1987).

[36] O.C. Zienkiewicz and D. Lefebvre, "A robust triangular plate bending element of the Reissner-Mindlin type", Int. J. Numer. Meth. Eng., 26, 1169 - 1184, (1988).

[37] O.C. Zienkiewicz, R.L. Taylor, P. Papadopoulos and E. Onate, "Plate bending elements with discrete constraints: New triangular elements", Computers & Structures, Vol. 35, No. 4, 505 - 522, (1990).

[38] G. Kirchhoff, "Über das Gleichgewicht und die Bewegung einer elastischen Scheibe", J. Reine Angew. Math. 40 (1850) 51-58.

[39] E. Reissner, "The effect of transverse shear deformation on the bending of elastic plates", J. Appl. Mech. 12 (1945) A69-A77.

[40] E. Reissner, "On bending of elastic plates", Quart. Appl. Math. 5, 55-68, (1947).

[41] R.D. Mindlin, "Influence of rotatory inertia and shear on flexural motions of isotropic elastic plates", J. Appl. Mech. 18, 31-38, (1951).

[42] H. Hencky, "Über die Berücksichtigung der Schubverzerrung in ebenen Platten", Ing. Arch. 16, 72-76, (1947).

[43] R. Piltner, "The derivation of a thick and thin plate formulation without ad hoc assumptions", Report No. UCB/SEMM-89/08, Department of Civil Engineering, University of California at Berkeley, 1989.

[44] R. Piltner, "Three-dimensional stress and displacement representations for plate problems", submitted for publication.

[45] S.N. Atluri, R.H. Gallagher and O.C. Zienkiewicz, (Eds.), "Hybrid and Mixed Finite Element Methods", Wiley & Sons, New York, 1983.

[46] R.H. Gallagher, "Finite Element Analysis: Fundamentals", Prentice-Hall, Englewood Cliffs, N.J., 1975.

[47] P. Tong and J.N. Rossettos, "Finite-Element Method - Basic Technique and Implementation", The MIT Press, Cambridge, 1977.

[48] O.C. Zienkiewicz, and R.L. Taylor, "The Finite Element Method", Volume 1: Basic Formulations and Linear Problems, McGraw-Hill, London, New York, 1989

[49] T.H.H. Pian, "Reflections and remarks on hybrid and mixed finite element methods", Chapter 29, p. 565 - 241, in: Hybrid and Mixed Finite Element Methods, (Eds.: S.N. Atluri, R.H. Gallagher and O.C. Zienkiewicz), Wiley & Sons, New York, 1983.

[50] T.H.H. Pian, "Derivation of element stiffness matrices by assumed stress distributions", AIAA Journal, 2, 1333 - 1336, (1964).

[51] T.H.H. Pian and K. Sumihara, "Rational approach for assumed stress elements", Int. J. Numer. Meth. Eng., 20, 1685 - 1695, (1984).

[52] T.H.H. Pian and C.C. Wu, "A rational approach for assuming stress terms for hybrid finite element formulations", Int. J. Numer. Meth. Eng., 26, 2331 - 2343, (1988).

[53] E. Trefftz, "Ein Gegenstück zum Ritzschen Verfahren", 2. Int. Kongr. f. Techn. Mechanik, Zürich 1926, 131 - 137

[54] E. Stein, "Die Kombination des modifizierten Trefftzschen Verfahrens mit der Methode der finiten Elemente", pp. 172 - 185, in: Finite Elemente in der Statik, Verlag Ernst + Sohn, Berlin, 1973

[55] G. Ruoff, "Die praktische Berechnung der Kopplungsmatrizen bei der Kombination der Trefftzschen Methode und der Methode der finiten Elemente", pp. 242 - 259, in: Finite Elemente in der Statik, Verlag Ernst + Sohn, Berlin, 1973

[56] O.C. Zienkiewicz, D.W. Kelly, and P. Bettess, "The coupling of finite element and boundary solution procedures", Int. J. Numer. Meth. Eng., 11, 355 - 376, (1977).

[57] O.C. Zienkiewicz, D.W. Kelly, and P. Bettess, "Marriage a la mode - the best of both worlds (finite elements and boundary integrals)", Proc. Int. Symp. on Innovative Numerical Analysis in Applied Engineering Science, Versailles, May 1977, pp. 19 - 26. Also, Ch. 5, pp. 81 - 106 in: Energy Methods in Finite Element Analysis, (Eds. R. Glowinski, E.Y. Rodin and O.C. Zienkiewicz), Wiley, New York, 1979

[58] A.P. Zielinski, and O.C. Zienkiewicz, "Generalized finite element analysis with T-complete boundary solution functions", Int. J. Numer. Meth. Eng., 21, 509 - 528, (1985).

[59] J. Jirousek, "Basis for development of large finite elements locally satisfying all field equations", Comp. Meth. Appl. Mech. Eng., 14, 65 - 92, (1978).

[60] J. Jirousek, "Implementation of local effects into conventional and non conventional finite element formulations", pp. 279 - 298, in: Local Effects in the Analysis of Structures, (Ed. P. Ladeveze), Elsevier Science Publishers, 1985.

[61] J. Jirousek, "The hybrid-Trefftz model - a finite element model with special suitability to adoptive solutions and local effect calculations", pp. 219 - 243, in: Finite Element Methods for Plate and Shell Structures, Volume 2: Formulations and Algorithms, Edited by T.J.R. Hughes and E. Hinton, Pineridge Press, Swansea, 1986.

[62] J. Jirousek, and L. Guex, "The hybrid-Trefftz finite element model and its application to plate bending", Int. J. Numer. Methods Eng., 23, 651 - 693, (1986).

[63] R. Piltner, "Spezielle finite Elemente mit Löchern, Ecken und Rissen unter Verwendung von analytischen Teillösungen", Doctoral Thesis, Ruhr-Universität Bochum, Fortschr.-Ber. VDI-Z. Reihe 1 Nr. 96, VDI-Verlag, Düsseldorf, 1982.

[64] R. Piltner, "Special finite elements with holes and internal cracks", Int. J. Numer. Meth. Eng., 21, 1471 - 1485, (1985).

[65] R. Piltner, "Finite Elemente mit Ansätzen im Trefftz'schen Sinne", pp. 267 - 278, in: Finite Elemente - Anwendung in der Baupraxis, (Eds. H. Grundmann, E. Stein, W. Wunderlich), Verlag Ernst + Sohn, Berlin/ München/ Düsseldorf , 1985.

[66] R. Piltner, "Special finite elements for an appropriate treatment of local effects", pp. 299 - 314, in: Local Effects in the Analysis of Structures, (Ed. P. Ladeveze), Elsevier Science Publishers, 1985.

[67] R. Piltner and R.L. Taylor, "The evaluation of stiffness matrices for elasticity problems with the aid of boundary integrals", pp. 38 - 45 in: "NUMETA 90: Numerical Methods in Engineering: Theory and Applications", (Eds. G.N. Pande, J. Middleton), Elsevier, London/New York, 1990.

[68] P. Tong, T.H.H. Pian, and S. Lasry, "A hybrid element approach to crack problems in plane elasticity", Int. J. Numer. Meth. Eng., 7, 297 - 308, (1973).

[69] MACSYMA Reference Manual, Version 10. The Mathlab Group, Laboratory for Computer Science, MIT (1983).

[70] R.H. Rand, "Computer Algebra in Applied Mathematics: An Introduction to MACSYMA", Pitman, Boston/London, 1984.

[71] S. Timoshenko, "Theory of Plates and Shells", McGraw-Hill, New York/London, 1940.

[72] R. Piltner and R.L. Taylor, "A boundary element algorithm using compatible boundary displacements and tractions", Int. J. Numer. Meth. Eng., 29, 1323 - 1341, (1990).

[73] R. Piltner and R.L. Taylor, "A boundary element algorithm for plate bending problems based on Cauchy's integral formula", Proceedings of the International Symposium on Boundary Element Methods, United Technologies Research Center, East Hartford, Connecticut, USA, October 1989, Springer, Berlin, Heidelberg, New York (to appear)